IEEE Access
Multidisciplinary | Rapid Review | Open Access Journal

Received January 5, 2022, accepted January 24, 2022, date of publication January 31, 2022, date of current version February 9, 2022.

Digital Object Identifier 10.1109/ACCESS.2022.3147817

Novel Resistive Distance Descriptors on Complex Network

MIN LI[1,3], SHUMING ZHOU[2], GAOLIN CHEN[1,2], WEI LIN[3], AND QIANRU ZHOU[2]
[1]College of Computer and Cyber Security, Fujian Normal University, Fuzhou, Fujian 350117, China
[2]School of Mathematics and Statistics, Fujian Normal University, Fuzhou, Fujian 350117, China
[3]Concord University College, Fujian Normal University, Fuzhou, Fujian 350117, China

Corresponding authors: Shuming Zhou (zhoushuming@fjnu.edu.cn) and Gaolin Chen (gaolinchen@fjnu.edu.cn)

This work was supported in part by the National Natural Science Foundation of China under Grant 61977016 and Grant 61572010, in part by the Natural Science Foundation of Fujian Province under Grant 2020J01164 and Grant 2017J01738, and in part by the Education and Scientific Research Project for Young and Middle-aged Teachers of Fujian Province under Grant JAT191119.

ABSTRACT Large-scale complex network data poses significant challenges for the analytic ideas and tools to monitor and analyze complex networks. As classical structure descriptors, average path length (L), global and local network efficiency (E_{glob} and E_{loc}), general and loop clustering coefficient (C_3 and D), play significant roles in complex network analysis. In this paper, we make use of resistive distance instead of the shortest path distance to suggest resistive distance descriptors, i.e., L_r, Ω_{glob} and Ω_{loc}, Ω_3 and D_r. We investigate all the resistive descriptors on classical WS, BA and ER models and find some interesting phenomenons. On one hand, L_r and Ω_3 (resp., Ω_{glob} and Ω_{loc}) can be used to characterize the features of small-word networks. On the other hand, L_r, Ω_3, and Ω_{glob} can be utilized to measure network invulnerability. To access the effectiveness of the resistive distance descriptors, we conduct extensive numerical simulations on synthetic and real networks. In comparison with the baselines, the proposed metrics show competitive performance on classical network models and are more efficient for networks with small and medium size.

INDEX TERMS Resistive distance, clustering coefficient, network efficiency, network invulnerability.

I. INTRODUCTION

During the last decades, network science, as a mature interdisciplinary field, has gained considerable attentions. Complex networks describe a wide range of systems in nature and society, such as biological, social, economic, power, traffic systems. These complex systems, which show nontrivial characteristics, are neither absolutely random nor perfectly regular. The statistical analysis of graphs, as a field of mathematics, plays an important role to understand real-world systems. The three influential statistical graph models, Barabási-Albert model (BA) [1], Watts-Strogatz model (WS) [2] and Erdös-Rényi model (ER) [3], are introduced to generate graphs and to predict some of their topological properties, such as degree distribution, average path length, clustering coefficient. Small-world networks, in terms of WS models, present two significant features of large clustering coefficient and short average path length. Scale-free networks, illustrated by BA models, emphasized that the degrees of nodes follow a power law distribution. An ER random network is also known as a binomial network, whose clustering coefficient is equal to its probability for edge creation.

In recent years, the researches of malicious attacks on complex networks have attracted great attentions. Malicious attacks can cause serious failures on various networks, such as traffic network [4], power grid network [5], supply chain network [6], etc. Many network security problems in the real world can be attributed to the invulnerability problem of the networks in terms of cascade failures. Generally, the invulnerability of networks is tightly related to their topological structures. The Scale-free network is robust under the random attack, while vulnerable under the high degree nodes attack [7]. Jalili [8] investigated how the small-worldness of networks changed when nodes are removed randomly or systematically. The network metrics, such as network efficiency, the size of the largest connected component, average path length, clustering coefficient, are commonly used to monitor network invulnerability. The clustering coefficient, introduced by Watts and Strogatz [2] to measure how tightly a node's neighbors are connected with each other, is an

The associate editor coordinating the review of this manuscript and approving it for publication was Chun-Hao Chen.

important statistical tool to describe the structure of complex networks. The concept of efficiency of a network, introduced by Latora and Marchiori [9], is to measure how it exchanges information efficiently. The efficiency ϵ_{ij}, between nodes i and j, is inversely proportional to the shortest path distance d_{ij}, denoted by $\epsilon_{ij} = \frac{1}{d_{ij}}$. By using efficiency measure, the small-world behavior can be interpreted and the small-world network is shown to be both locally and globally efficient.

As an interesting notion of distance on graphs, resistive distance, proposed by Klein and Randić [10] based on an electrical-theoretic approach in 1993, has been investigated by Stephenson and Zelen [11] in 1989 in terms of information-theoretic approach. Let a network be viewed as an electrical circuit, where each edge corresponds to a resistor and each node is a junction between resistors. Consider that a unit current enters at source i and leaves from target j. Effective resistance r_{ij}, between i and j, can be denoted by potential difference between them. A high potential difference between nodes i and j means that i and j are far away. In fact, r_{ij} satisfies non-negativity, symmetry and triangle inequality and can be viewed as a distance function. Note that $r_{ij} \leq d_{ij}$, with equality if and only if there is only one path from i to j, where d_{ij} represents the shortest path distance between i and j. Refer to [12]–[15] for different calculation methods of resistive distance. A main topic about resistance distance is its calculation in various graphs. Relevant literatures are available in [16]–[18]. In recent years, many scholars have studied resistive distance in different aspects of complex network, such as community detection [19]–[23], centrality measures [24]–[26], link prediction [27] and network robustness [28]–[31], etc. By the way, resistance in the network is intimately connected with the lengths of random walks on the graph. For any i and j, $T_{ij} = 2mr_{ij}$, where m is the number of edges of the G, T_{ij} indicates the commute time and r_{ij} represents the resistive distance. Refer to [32] for more details.

In this paper, we aim to design novel descriptors using resistive distance instead of the shortest path distance. To sum up, our contributions are summarized as follows:

- Novel resistive descriptors, shown in Table 1, are suggested to explore on classical WS, BA and ER models.
- Motivated by L and C_3 (resp., E_{glob} and E_{loc}), L_r and Ω_3 (resp., Ω_{glob} and Ω_{loc}) are employed to characterize small-world networks.
- In comparison of L, C_3 and E_{glob}, L_r, Ω_3 and Ω_{glob} are utilized to measure network invulnerability and the Kendall's Tau coefficient is utilized to analyze each resistive descriptor's correlations with that based on shortest path length.

The rest of the paper proceeds as follows. Section 2 reviews classic network descriptors and a brief overview of resistive distance. Next, we introduce several novel structure descriptors based on resistive distance in Section 3. Section 4 presents the algorithm descriptions and Section 5 shows experiment results and analysis. Finally, Section 6 concludes this paper with a summary and proposes future directions.

TABLE 1. The mainly discussed network descriptors in this work, are shown based on the shortest path distance and resistive path distance, respectively.

shortest-path	resistive-path	Description
Wr	Kf	Total distance of the graph.
L	L_r	Average path length.
E_{glob}	Ω_{glob}	Global efficiency.
E_{loc}	Ω_{loc}	Local efficiency based on G_i.
$E_{loc'}$	$\Omega_{loc'}$	Local efficiency based on $\hat{G}_i$.
C_3	Ω_3	Clustering coefficient.
D	D_r	Loop coefficient.

TABLE 2. Summary of main notations.

notations	descriptions
G	A simple undirected and connected graph.
N	Network size.
k_i	The degree of node i.
Γ_i	The set of neighbors of node i.
d_{ij}	The shortest path distance between node i and j.
r_{ij}	The resistive path distance between node i and j.
$d_{jk/i}$	The shortest path distance between j and k not passing through i.
L_G	Laplacian matrix of G.
D_G	Degree matrix of G.
A_G	Adjacency matrix of G.
$R_m(G)$	Resistive distance matrix of G.
$D_m(G)$	Shortest path distance matrix of G.
τ	Kendall's Tau correlation coefficient.
G_i	The induced subgraph of open neighborhood of i.
$\hat{G}_i$	The induced subgraph of closed neighborhood of i.
$D(i)$	The loop coefficient of an arbitrary node i.
$R(i)$	The cyclic coefficient of node i.
$C_3(i)$	The clustering coefficient of node i.
$C_4(i)$	Quadrilateral coefficient of node i.
$SC(i)$	Subgraph centrality of node i.
$\bar{\lambda}$	Natural connectivity of G.
$C_3(G)$	The average clustering coefficient of G.

II. PRELIMINARIES

A complex network can be described as a graph $G = (V, E)$, where V denotes the set of nodes and E represents the set of edges. The Laplacian matrix $L_G = D_G - A_G$, where D_G is the degree matrix with $(D_G)_{ii} = k_i$, and A_G indicates the adjacency matrix, with $(A_G)_{ij} = 1$ when an edge (i, j) exists and $(A_G)_{ij} = 0$ otherwise.

In this paper, unless differently stated, G represents a connected, undirected and unweighted graph without self-loops and multiple links. Ordinarily, N denotes network size. k_i, Γ_i and G_i indicate the degree, the set of neighbors and the induced subgraph of open neighborhood of node i, respectively. d_{ij} and r_{ij} represent the shortest path distance and resistive path distance between node i and j, respectively. Summary of main notations are shown in Table 2.

A. CLASSIC NETWORK DESCRIPTORS

In this section, we introduce some commonly used global and local statistical descriptors of complex network, i.e., wiener index (Wr), average path length (L), global efficiency (E_{glob}),

local efficiency (E_{loc}), clustering coefficient (C_3), quadrilateral coefficient (C_4), cyclic coefficient (R), loop coefficient (D), subgraph centrality (SC) and natural connectivity ($\bar{\lambda}$). These descriptors will be used as baselines for comparison in experimental section.

- Wiener index (Wr) [33]
  The Wiener index of a graph is the sum of the shortest-path distances between each pair of reachable nodes, i.e.,
  $$Wr = \sum_{i<j} d_{ij}, \tag{1}$$
  where d_{ij} is the shortest path distance between i and j. The Wiener index is one of the well-known distance-based molecular structure descriptors, which can be used for modeling physical, pharmacologic, biological and other properties of chemical compounds.
- Average path length (L) [2]
  The average path length L denotes the average distance between two generic nodes, i.e.,
  $$L = \frac{1}{N(N-1)} \sum_{i \neq j \in G} d_{ij}, \tag{2}$$
  where d_{ij} indicates the shortest path distance between i and j and N is the number of nodes of G. Many real world networks (graphs) are observed to be small worlds, i.e., the average path length among nodes is small.
- Global efficiency (E_{glob}) [9]
  The global efficiency of G, denoted by $E_{glob}(G)$, is defined as
  $$E_{glob}(G) = \frac{1}{N(N-1)} \sum_{i \neq j \in G} \frac{1}{d_{ij}}, \tag{3}$$
  where d_{ij} indicates the shortest path distance between i and j and N is the number of nodes of G. E_{glob} quantifies the exchange of information across the whole network on a global scale, where information is concurrently exchanged.
- Local efficiency (E_{loc}) [9]
  The local efficiency of node i, denoted by $E_{loc}(i)$, i.e.,
  $$E_{loc}(i) = E_{glob}(G_i), \tag{4}$$
  where G_i represents the induced subgraph of open neighborhood of node i. The local efficiency $E_{loc}(i)$ quantifies a network's resistance to failure on a small scale. The average local efficiency of G, denoted by $E_{loc}(G)$, i.e.,
  $$E_{loc}(G) = \frac{1}{N} \sum_{i \in G} E_{loc}(i) = \frac{1}{N} \sum_{i \in G} E_{glob}(G_i). \tag{5}$$
- Clustering coefficient (C_3) [2]
  The clustering coefficient of node i, denoted by $C_3(i)$, i.e.,
  $$C_3(i) = \frac{2}{k_i(k_i-1)} \sum_{j \neq k} \sum_{\in \Gamma_i} n_{jk}. \tag{6}$$
  Here, k_i and Γ_i indicate the degree and the set of neighbors of node i, respectively. n_{jk}=1 if there is a link between j and k, and n_{jk}=0 otherwise. $C_3(i)$ gives the ratio of the existing number of links between the neighbors of node i and its maximum possible number $k_i(k_i-1)/2$. $C_3(G)$ denotes the average clustering coefficient of G.
- Quadrilateral coefficient (C_4) [34]
  The quadrilateral coefficient of node i, is denoted by $C_4(i)$, i.e.,
  $$C_4(i) = \frac{\sum_{m=1}^{k_i} \sum_{n=m+1}^{k_i} q_i(m,n))}{\sum_{m=1}^{k_i} \sum_{n=m+1}^{k_i} [a_i(m,n) + q_i(m,n)]}, \tag{7}$$
  where m and n are neighbors of the node i, $q_i(m,n)$ are the number of common neighbors between m and n, and $a_i(m,n) = (k_m - \eta_i(m,n))(k_n - \eta_i(m,n))$ with $\eta_i(m,n) = 1 + q_i(m,n) + \theta_{mn}$, where
  $$\theta_{mn} = \begin{cases} 1, & (m,n) \in E, \\ 0, & otherwise. \end{cases} \tag{8}$$
  C_4 gives the probability that two neighbors of node i share a common neighbor, which is different from i. $C_4(G)$ denotes the average quadrilateral coefficient of G.
- Cyclic coefficient (R) [37] The cyclic coefficient of node i, is denoted by $R(i)$, i.e.,
  $$R(i) = \frac{2}{k_i(k_i-1)} \sum_{\langle lm \rangle} \frac{1}{S_{lm}^i}, \tag{9}$$
  where k_i indicates the degree of node i and $\langle lm \rangle$ denotes all the pairs of the neighbors of the node i. S_{lm}^i is the size of the smallest loop passing through node i and its pair of neighbors $\langle l, m \rangle$. R can characterize the cyclic structures of complex networks and it takes values between 0 and 1/3. If the network is a perfect tree-like structure, $R = 0$. The larger value of R indicates that the network is more cyclic. $R(G)$ denotes the average cyclic coefficient of G.
- Loop coefficient (D) [38] The loop coefficient of an arbitrary node i is denoted by
  $$D(i) = \frac{2}{k_i(k_i-1)} \sum_{j \neq k} \sum_{\in \Gamma_i} \frac{1}{d_{jk/i}}, \tag{10}$$
  where k_i represents the degree of i, Γ_i indicates the set of neighbors of node i, and $d_{jk/i}$ is the length of shortest path between j and k not passing through i. Loop coefficient varies from 0 to 1. In addition, $D(i)$ coincides with $C_3(i)$, if only the shortest paths $d_{jk/i}$=1 are taken into account. Therefore, Loop coefficient is a generalization of the clustering coefficient. $D(G)$ denotes the average loop coefficient of G.
- Subgraph centrality (SC) [35] The subgraph centrality of an arbitrary node i is denoted by
  $$SC(i) = \sum_{j=1}^{N} (v_j^i)^2 e^{\lambda_j}, \tag{11}$$

where v_j is an eigenvector of the adjacency matrix A of G corresponding to the eigenvalue λ_j. Furthermore, the average subgraph centrality of G is denoted by

$$\langle SC\rangle = \frac{1}{N}\sum_{i=1}^{N} SC(i) = \frac{1}{N}\sum_{i=1}^{N} e^{\lambda_i}. \tag{12}$$

By the way, natural connectivity $\bar{\lambda}$ [36] of G, which is highly correlated with subgraph centrality, is denoted by

$$\bar{\lambda} = \ln\left[\langle SC\rangle\right] = \ln\left[\frac{1}{N}\sum_{i=1}^{N} e^{\lambda_i}\right]. \tag{13}$$

Natural connectivity (resp., subgraph centrality), as a measure of structure robustness in complex networks, characterizes the redundancy of alternative routes in a network by quantifying the weighted number of closed walks of all lengths.

B. EFFECTIVE RESISTANCE

An electrical network is defined as $N = (G, r) = (V, E, r)$, where r is a function: $E \to R^+$, and r_e denotes the resistance of the edge e. Also, we define an electrical network in the form $N = (G, c)$, where c is the a conductance function, and $c_e = 1/r_e$ represents the conductance of the edge e. For any $e \in E$, if $r_e = 1$, we call the electrical network simple.

Klein and Randić [10] have proved that the effective resistance is indeed a distance function. Previous studies [10], [12], [14], [25] have shown that Laplacian matrix L_G plays a vital role in the theory of the resistive distance. In this work, the resistive matrix of G is defined as $R_m(G)$ and its calculation is shown in algorithm 1 [39]. All the proposed resistive descriptors are calculated based on $R_m(G)$. Here, we will give some related results from [10].

Definition 1 [10]: The total effective resistance, also called Kirchhoff index, is the sum of the effective resistance over all pairs of nodes in G:

$$Kf = \sum_{i<j} r_{ij}. \tag{14}$$

It can be expressed in terms of Laplacian eigenvalues as follows:

$$Kf = n\sum_{k=2}^{n} \frac{1}{\mu_k}, \tag{15}$$

where $\mu_1 < \mu_2 \le \cdots \le \mu_n$ are the eigenvalues of Laplacian matrix L.

Theorem 2 [10]: For all distinct pairs of nodes i, j in G, $d_{ij} \ge r_{ij}$, with equality if there is only one path between i and j.

Corollary 3 [10]: If G is a tree, the conventional distance is the same as the effective resistance distance, i.e., $d_{ij} = r_{ij}$.

III. NOVEL NETWORK DESCRIPTORS BASED ON RESISTIVE DISTANCE

A. AVERAGE PATH LENGTH BASED ON RESISTIVE DISTANCE

Definition 4 (L_r): The average path length of G is denoted by L_r, i.e.,

$$L_r = \frac{1}{N(N-1)}\sum_{i\neq j\in G} r_{ij}. \tag{16}$$

Equivalently,

$$L_r = \frac{2}{N(N-1)}Kf. \tag{17}$$

B. EFFICIENCY DESCRIPTORS BASED ON RESISTIVE DISTANCE

Definition 5 (Ω_{glob}): The global efficiency of G is denoted by $\Omega_{glob}(G)$, i.e.,

$$\Omega_{glob}(G) = \frac{1}{N(N-1)}\sum_{i\neq j\in G}\frac{1}{r_{ij}}. \tag{18}$$

Definition 6 (Ω_{loc}): The local efficiency of node i is denoted by $\Omega_{loc}(i)$, i.e.,

$$\Omega_{loc}(i) = \Omega_{glob}(G_i), \tag{19}$$

where G_i is the induced subgraph of neighbors of i such that $i \notin G_i$. Usually, G_i is a disconnected graph. For any $j, k \in G_i$, when there is no path between j and k, we define $r_{jk} = +\infty$, i.e., $\frac{1}{r_{jk}} = 0$. Besides, the local efficiency of G is denoted by $\Omega_{loc}(G)$, i.e.,

$$\Omega_{loc}(G) = \frac{1}{N}\sum_{i\in G}\Omega_{loc}(i) = \frac{1}{N}\sum_{i\in G}\Omega_{glob}(G_i). \tag{20}$$

By the way, in this work, another local efficiency $\Omega_{loc'}$ is defined by

$$\Omega_{loc'}(i) = \Omega_{glob}(\hat{G}_i), \tag{21}$$

where $\hat{G}_i$ is the induced subgraph of neighbors of i such that $i \in \hat{G}_i$. $\Omega_{loc'}(G)$ indicates the average local efficiency of G. Similarly, the formula based on shortest paths distance is given by

$$E_{loc'}(i) = E_{glob}(\hat{G}_i). \tag{22}$$

Furthermore, $E_{loc'}(G)$ denotes the average local efficiency of G.

C. CLUSTERING COEFFICIENT BASED ON RESISTIVE DISTANCE

Definition 7 (Ω_3): The resistive clustering coefficient of an arbitrary node i is defined as

$$\Omega_3(i) = \frac{2}{k_i(k_i-1)}\sum_{j\neq k}\sum_{\in\Gamma_i}\eta_{jk}, \tag{23}$$

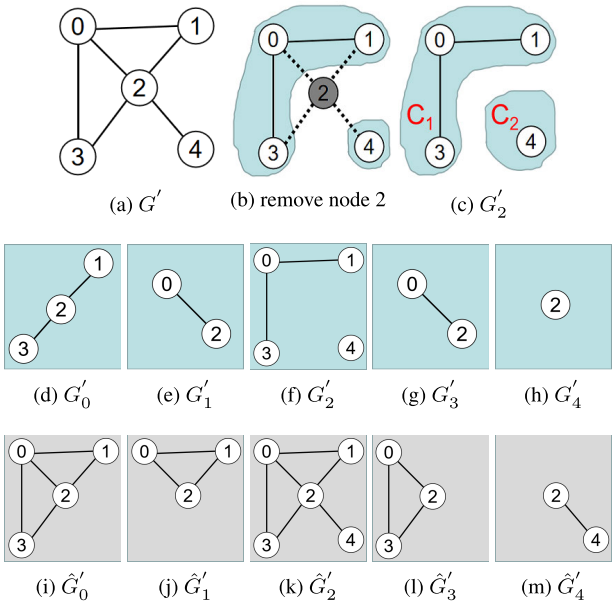

FIGURE 1. An example network G' with five nodes.

where $\eta_{jk} = r_{jk}$ if there is a link between j and k, and $\eta_{jk} = 0$ otherwise. $\Omega_3(G)$ denotes the average clustering coefficient of G in terms of resistive distance.

Definition 8 (D_r): The resistive loop coefficient of an arbitrary node i is defined as

$$D_r(i) = \frac{2}{k_i(k_i-1)} \sum_{j \neq k \in \Gamma_i} \frac{1}{r_{jk}}, \tag{24}$$

where $D_r(G)$ denotes the average resistive loop coefficient of G.

D. EXAMPLE EXPLANATION

Based on the above definitions, some simple examples are presented to explain how the proposed descriptors work in a specific network.

1) THE FIRST EXAMPLE

As shown in Figure 1 (a), a simple G' is given. Figure 1 (d)-(h) represent the induced subgraphs G'_i of open neighborhood of i, while Figure 1 (i)-(m) show the induced subgraphs $\hat{G}'_i$ of close neighborhood of i. Figure 1 (b) and (c) describe how to obtain G'_2.

At first, we calculate W_r, L, $E_{glob}(G')$, Kf, L_r and $\Omega_{glob}(G')$. The matrix of the shortest path distance of G' is

$$D_m[G'] = \begin{array}{c} \\ 0 \\ 1 \\ 2 \\ 3 \\ 4 \end{array} \begin{array}{c} \begin{array}{ccccc} 0 & 1 & 2 & 3 & 4 \end{array} \\ \begin{pmatrix} 0 & 1 & 1 & 1 & 2 \\ 1 & 0 & 1 & 2 & 2 \\ 1 & 1 & 0 & 1 & 1 \\ 1 & 2 & 1 & 0 & 2 \\ 2 & 2 & 1 & 2 & 0 \end{pmatrix} \end{array}.$$

According to Eq. (1) and $D_m[G']$,

$$\begin{aligned} W_r &= \sum_{i<j} d_{ij} \\ &= d_{01} + d_{02} + d_{03} + d_{04} + d_{12} + d_{13} \\ &\quad + d_{14} + d_{23} + d_{24} + d_{34} \\ &= 1 + 1 + 1 + 2 + 1 + 2 + 2 + 1 + 1 + 2 \\ &= 14. \end{aligned}$$

According to Eq. (2) and $D_m[G']$,

$$L = \frac{2}{N(N-1)} W_r = 1.4.$$

According to Eq. (3) and $D_m[G']$,

$$\begin{aligned} E_{glob}(G') &= \frac{1}{N(N-1)} \sum_{i \neq j \in G'} \frac{1}{d_{ij}} \\ &= \frac{2}{[5*(5-1)]} \left(\frac{1}{d_{01}} + \frac{1}{d_{02}} + \frac{1}{d_{03}} + \frac{1}{d_{04}} \right. \\ &\quad \left. + \frac{1}{d_{12}} + \frac{1}{d_{13}} + \frac{1}{d_{14}} + \frac{1}{d_{23}} + \frac{1}{d_{24}} + \frac{1}{d_{34}}\right) \\ &= 0.1\left(\frac{1}{1} + \frac{1}{1} + \frac{1}{1} + \frac{1}{2} \right. \\ &\quad \left. + \frac{1}{1} + \frac{1}{2} + \frac{1}{2} + \frac{1}{1} + \frac{1}{1} + \frac{1}{2}\right) \\ &= 0.8. \end{aligned}$$

In addition, according to algorithm 1, the resistive distance matrix of G' is

$$R_m[G'] = \begin{array}{c} \\ 0 \\ 1 \\ 2 \\ 3 \\ 4 \end{array} \begin{array}{c} \begin{array}{ccccc} 0 & 1 & 2 & 3 & 4 \end{array} \\ \begin{pmatrix} 0 & 0.62 & 0.5 & 0.62 & 1.5 \\ 0.62 & 0 & 0.62 & 1 & 1.63 \\ 0.5 & 0.62 & 0 & 0.62 & 1 \\ 0.62 & 1 & 0.62 & 0 & 1.63 \\ 1.5 & 1.63 & 1 & 1.63 & 0 \end{pmatrix} \end{array}.$$

According to Eq. (14) and $R_m[G']$,

$$\begin{aligned} Kf &= \sum_{i<j} r_{ij} \\ &= r_{01} + r_{02} + r_{03} + r_{04} + r_{12} \\ &\quad + r_{13} + r_{14} + r_{23} + r_{24} + r_{34} \\ &= 0.62 + 0.5 + 0.62 + 1.5 + 0.62 \\ &\quad + 1 + 1.63 + 0.62 + 1 + 1.63 \\ &= 9.74. \end{aligned}$$

According to Eq. (17) and $R_m[G']$,

$$L_r = \frac{2}{N(N-1)} Kf = 0.974.$$

According to Eq. (18) and $R_m[G']$,

$$\begin{aligned} \Omega_{glob}(G') &= \frac{1}{N(N-1)} \sum_{i \neq j \in G'} \frac{1}{r_{ij}} \\ &= \frac{2}{[5*(5-1)]} \left(\frac{1}{r_{01}} + \frac{1}{r_{02}} + \frac{1}{r_{03}} + \frac{1}{r_{04}} \right. \end{aligned}$$

$$
\begin{aligned}
&+\frac{1}{r_{12}}+\frac{1}{r_{13}}+\frac{1}{r_{14}}+\frac{1}{r_{23}}+\frac{1}{r_{24}}+\frac{1}{r_{34}})\\
&=0.1(\frac{1}{0.62}+\frac{1}{0.5}+\frac{1}{0.62}+\frac{1}{1.5}\\
&+\frac{1}{0.62}+\frac{1}{1}+\frac{1}{1.63}+\frac{1}{0.62}+\frac{1}{1}+\frac{1}{1.63})\\
&=1.23.
\end{aligned}
$$

Next, in terms of node 2, $E_{loc}(2)$, $\Omega_{loc}(2)$, $\Omega_3(2)$, $D_r(2)$, $E_{loc'}(2)$ and $\Omega_{loc'}(2)$ are computed below.

As shown in Figure 1 (b) and (c), remove node 2 from G' and obtain G'_2, which is the induced subgraph of neighbors of node 2. G'_2 has two components C_1 and C_2. As is well known, a graph is a tree if only if it is connected and has no loop. More than one tree can constitute a forest. Clearly, both C_1 and C_2 are trees, and C_2 is a trivial tree. G'_2 is a forest. According to Corollary 2.3, for any i and j of a tree, $r_{ij}=d_{ij}$. Thus, the distance matrix of G'_2 can be denoted as

$$
R_m[G'_2]=D_m[G'_2]=\begin{array}{c}\\0\\1\\3\\4\end{array}\begin{array}{c}\begin{array}{cccc}0&1&3&4\end{array}\\\begin{pmatrix}0&1&1&+\infty\\1&0&2&+\infty\\1&2&0&+\infty\\+\infty&+\infty&+\infty&+\infty\end{pmatrix}\end{array}.
$$

According to Eqs. (3)-(4) and $D_m[G'_2]$,

$$
\begin{aligned}
E_{loc}(2)&=E_{glob}(G'_2)\\
&=\frac{1}{N(N-1)}\sum_{i\neq j\in G'_2}\frac{1}{d_{ij}}\\
&=\frac{2}{[4*(4-1)]}(\frac{1}{d_{01}}+\frac{1}{d_{03}}+\frac{1}{d_{04}}\\
&+\frac{1}{d_{13}}+\frac{1}{d_{14}}+\frac{1}{d_{34}})\\
&=\frac{2}{12}(\frac{1}{1}+\frac{1}{1}+0+\frac{1}{2}+0+0)\\
&=0.42.
\end{aligned}
$$

Similarly, according to Eqs. (18)-(19) and $R_m[G'_2]$,

$$
\begin{aligned}
\Omega_{loc}(2)&=\Omega_{glob}(G'_2)\\
&=\frac{1}{N(N-1)}\sum_{i\neq j\in G'_2}\frac{1}{r_{ij}}\\
&=\frac{2}{[4*(4-1)]}(\frac{1}{r_{01}}+\frac{1}{r_{03}}\\
&+\frac{1}{r_{04}}+\frac{1}{r_{13}}+\frac{1}{r_{14}}+\frac{1}{r_{34}})\\
&=\frac{2}{12}(\frac{1}{1}+\frac{1}{1}+0+\frac{1}{2}+0+0)\\
&=0.42.
\end{aligned}
$$

In this example, for any $i\in G'$, G'_i is either a tree or a forest (see Figure 1 (d)-(h)). That is, only one shortest path exists between any pair of connected nodes in G'_i. In other words, the resistive distance equals to the shortest path distance between them. Thus, for any $i\in G'$, $\Omega_{loc}(i)=E_{loc}(i)$, which can be seen in Table 3.

Meanwhile, for node 2, $\Gamma_2=\{0,1,3,4\}$ and $k_2=4$. According to Eq. (23) and $R_m[G']$,

$$
\begin{aligned}
\Omega_3(2)&=\frac{2}{k_2(k_2-1)}\sum_{j\neq k}\sum_{\in\Gamma_2}\eta_{jk}\\
&=\frac{2}{[4*(4-1)]}(r_{01}+r_{03})\\
&=\frac{2}{[4*(4-1)]}(0.62+0.62)\\
&=0.21.
\end{aligned}
$$

According to Eq. (24) and $R_m[G']$,

$$
\begin{aligned}
D_r(2)&=\frac{2}{k_2(k_2-1)}\sum_{j\neq k\in\Gamma_2}\frac{1}{r_{jk}}\\
&=\frac{2}{[4*(4-1)]}(\frac{1}{r_{01}}+\frac{1}{r_{03}}\\
&+\frac{1}{r_{04}}+\frac{1}{r_{13}}+\frac{1}{r_{14}}+\frac{1}{r_{34}})\\
&=\frac{2}{[4*(4-1)]}(\frac{1}{0.62}+\frac{1}{0.62}\\
&+\frac{1}{1.5}+\frac{1}{1}+\frac{1}{1.63}+\frac{1}{1.63})\\
&=1.02.
\end{aligned}
$$

See Figure 1 (a) and (k), G' and $\hat{G}'_2$ represent the same graph. Thus, according to Eqs. (21) and (22),

$$
\Omega_{loc'}(2)=\Omega_{glob}(\hat{G}'_2)=\Omega_{glob}(G')=1.23,
$$

and,

$$
E_{loc'}(2)=E_{glob}(\hat{G}'_2)=E_{glob}(G')=0.8.
$$

We turn to calculate $\Omega_{loc'}(1)$ and $E_{loc'}(1)$. See Figure 1 (j) for $\hat{G}'_1$. The shortest path distance matrix and resistive distance matrix is

$$
D_m[\hat{G}'_1]=\begin{array}{c}\\0\\1\\2\end{array}\begin{array}{c}\begin{array}{ccc}0&1&2\end{array}\\\begin{pmatrix}0&1&1\\1&0&1\\1&1&0\end{pmatrix}\end{array},\ and
$$

$$
R_m[\hat{G}'_1]=\begin{array}{c}\\0\\1\\2\end{array}\begin{array}{c}\begin{array}{ccc}0&1&2\end{array}\\\begin{pmatrix}0&2/3&2/3\\2/3&0&2/3\\2/3&2/3&0\end{pmatrix}\end{array}.
$$

Then, in terms of $D_m[\hat{G}'_1]$ and $R_m[\hat{G}'_1]$,

$$
E_{loc'}(1)=E_{glob}(\hat{G}'_1)=\frac{2}{3(3-1)}(1+1+1)=1,
$$

and,

$$
\Omega_{loc'}(1)=\Omega_{glob}(\hat{G}'_1)=\frac{2}{3(3-1)}(\frac{3}{2}+\frac{3}{2}+\frac{3}{2})=1.5.
$$

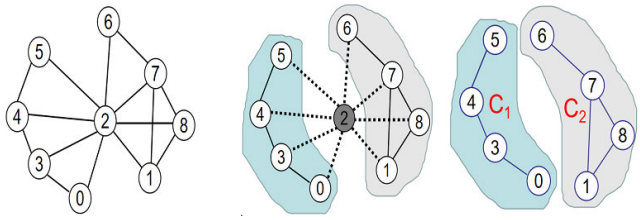

(a) G'' (b) remove node 2 (c) G_2''

FIGURE 2. An example network with nine nodes.

2) THE SECOND EXAMPLE

Next, let us turn to Figure 2 (a), which displays another example network named G''. When node 2 of G'' is removed (see Figure 2 (b)), two connected components are obtained. Note that, the component under grey background owns cycles. Thus, not all the pairs of nodes have only one path. For instance, we can find only one path between 6 and 7, i.e., 6-7. However, two paths, indicated by 6-7-8 and 6-7-1-8, exist between 6 and 8. Therefore, Ω_{loc} must be different from E_{loc} for G''. Here, we give detailed computations of $E_{loc}(2)$ and $\Omega_{loc}(2)$ of G''. After node 2 and all directed links incident with it are removed, G_2'', i.e., the induced graph of neighbors of node 2, is obtained. The shortest path distance matrix of G_2'' is, $D_m[G_2'']$, as shown at the bottom of the page.

According to Eqs. (3)-(4) and $D_m[G_2'']$,

$$\begin{aligned} E_{loc}(2) &= E_{glob}(G_2'') \\ &= \frac{2}{[8*(8-1)]}\Big(\frac{1}{d_{03}}+\frac{1}{d_{04}}+\frac{1}{d_{05}}+\frac{1}{d_{34}}+\frac{1}{d_{35}} \\ &\quad +\frac{1}{d_{45}}+\frac{1}{d_{67}}+\frac{1}{d_{68}}+\frac{1}{d_{61}}+\frac{1}{d_{78}}+\frac{1}{d_{71}}+\frac{1}{d_{81}}\Big) \\ &= \frac{2}{[8*(8-1)]}\Big(\frac{1}{1}+\frac{1}{2}+\frac{1}{3}+\frac{1}{1}+\frac{1}{2}+\frac{1}{1} \\ &\quad +\frac{1}{1}+\frac{1}{2}+\frac{1}{2}+\frac{1}{1}+\frac{1}{1}+\frac{1}{1}\Big) \\ &= 0.33. \end{aligned}$$

In contrast, the resistive matrix of G_2'' is, $R_m[G_2'']$, as shown at the bottom of the next page.

Similarly, according to Eqs. (18)-(19) and $R_m[G_2'']$,

$$\begin{aligned} \Omega_{loc}(2) &= \Omega_{glob}(G_2'') \\ &= \frac{2}{[8*(8-1)]}\Big(\frac{1}{r_{03}}+\frac{1}{r_{04}}+\frac{1}{r_{05}}+\frac{1}{r_{34}}+\frac{1}{r_{35}} \\ &\quad +\frac{1}{r_{45}}+\frac{1}{r_{67}}+\frac{1}{r_{68}}+\frac{1}{r_{61}}+\frac{1}{r_{78}}+\frac{1}{r_{71}}+\frac{1}{r_{81}}\Big) \\ &= \frac{2}{[8*(8-1)]}\Big(\frac{1}{1}+\frac{1}{2}+\frac{1}{3}+\frac{1}{1}+\frac{1}{2}+\frac{1}{1} \\ &\quad +\frac{1}{1}+\frac{1}{1.67}+\frac{1}{1.67}+\frac{1}{0.67}+\frac{1}{0.67}+\frac{1}{0.67}\Big) \\ &= 0.39. \end{aligned}$$

For the sake of simplicity, other descriptors's details are omitted in this example, whose results are also shown in Table 3. Moreover, the proposed descriptors are labelled in bold.

IV. ALGORITHM DESCRIPTION

All the resistive quantities in this work are calculated in algorithms 1-6, respectively.

Algorithm 1 *CalculateR*

Input: $G(V, E)$
Output: $R_m(G)$
1: $n = |G(V, E)|$;
2: $A_G = adjacency\_matrix(G)$;
3: $D_G = degree\_matrix(A_G)$;
4: $L_G = D_G - A_G$;
5: $J = ||1||$;
6: $X = ||x_{ij}|| = (L + \frac{1}{n}J)^{-1}$;
7: $\widetilde{X} = diag(x_{11}, \ldots, x_{nn})$;
8: $R_m(G) = ||r_{ij}|| = \widetilde{X}J + J\widetilde{X} - 2X$;

Algorithm 2 *CalculateKf*

Input: $G(V, E)$
Output: Kf
1: $\mu List = laplacian\_spectrum(G)$;
// $\mu List = [\mu_1 = 0, \mu_2, \ldots, \mu_n]$;
2: $Kf = n\sum_{k=2}^{n}\frac{1}{\mu_k}$;

The calculation method of resistive matrix is shown in algorithm 1. The input is a graph G and the output $R_m(G)$

$$D_m[G_2''] = \begin{array}{c} \\ 0 \\ 3 \\ 4 \\ 5 \\ 6 \\ 7 \\ 8 \\ 1 \end{array} \begin{array}{c} \begin{array}{cccccccc} 0 & 3 & 4 & 5 & 6 & 7 & 8 & 1 \end{array} \\ \begin{pmatrix} 0 & 1 & 2 & 3 & +\infty & +\infty & +\infty & +\infty \\ 1 & 0 & 1 & 2 & +\infty & +\infty & +\infty & +\infty \\ 2 & 1 & 0 & 1 & +\infty & +\infty & +\infty & +\infty \\ 3 & 2 & 1 & 0 & +\infty & +\infty & +\infty & +\infty \\ +\infty & +\infty & +\infty & +\infty & 0 & 1 & 2 & 2 \\ +\infty & +\infty & +\infty & +\infty & 1 & 0 & 1 & 1 \\ +\infty & +\infty & +\infty & +\infty & 2 & 1 & 0 & 1 \\ +\infty & +\infty & +\infty & +\infty & 2 & 1 & 1 & 0 \end{pmatrix} \end{array}.$$

TABLE 3. The values of four local efficiency quantities on two example networks.

Metrics	G'					G''								
	0	1	2	3	4	0	1	2	3	4	5	6	7	8
E_{loc}	0.83	1.0	0.42	1.0	0	1.0	1.0	0.33	0.83	0.83	1.0	1.0	0.83	1.0
Ω_{loc}	**0.83**	**1.0**	**0.42**	**1.0**	**0**	**1.0**	**1.5**	**0.39**	**0.83**	**0.83**	**1.0**	**1.0**	**1.12**	**1.5**
$E_{loc'}$	0.92	1.0	0.8	1.0	1.0	1.0	1.0	0.71	0.92	0.92	1.0	1.0	0.9	1.0
$\Omega_{loc'}$	**1.57**	**1.5**	**1.23**	**1.5**	**1.0**	**1.5**	**2.0**	**1.38**	**1.57**	**1.57**	**1.5**	**1.5**	**1.85**	**2.0**
SC	4.36	3.10	5.21	3.10	1.74	3.79	6.63	16.92	5.47	5.47	3.79	4.11	8.48	6.63
C_4	1.0	1.0	1.0	1.0	0	1.0	1.0	0.12	1.0	1.0	1.0	1.0	1.0	1.0
C_3	0.67	1.0	0.33	1.0	0	1.0	1.0	0.25	0.67	0.67	1.0	1.0	0.67	1.0
Ω_3	**0.41**	**0.5**	**0.21**	**0.5**	**0**	**0.48**	**0.45**	**0.14**	**0.37**	**0.37**	**0.48**	**0.4**	**0.34**	**0.45**
D	0.83	1.0	0.42	1.0	0	1.0	1.0	0.48	0.83	0.83	1.0	1.0	0.83	1.0
R	0.31	0.33	0.15	0.33	0	0.33	0.33	0.22	0.31	0.31	0.33	0.33	0.31	0.33
D_r	**1.41**	**2.0**	**1.02**	**2.0**	**0**	**2.08**	**2.22**	**1.21**	**1.60**	**1.60**	**2.08**	**2.5**	**1.68**	**2.22**

Algorithm 3 *Calculate*L_r

Input: $G(V, E)$
Output: L_r
1: $n = |G(V, E)|$;
2: $R_m(G) = calculateR(G)$;
3: $sumL = 0$;
4: $numList = [0, 1, \ldots, n-1]$;
5: **for** i in $numList$ **do**
6: **for** j in $numList$ **do**
7: $sumL = sumL + R_m[i, j]$;
8: **end for**
9: **end for**
10: $L_r = sumL/[n * (n-1)]$;

Algorithm 4 *Calculate*Ω_{glob}

Input: $G(V, E)$
Output: Ω_{glob}
1: $n = |G(V, E)|$;
2: $R_m(G) = calculateR(G)$;
3: $sum\Omega = 0$;
4: $numList = [0, 1, \ldots, n-1]$;
5: **for** i in $numList$ **do**
6: **for** j in $numList$ **do**
7: **if** $i \neq j$ **then**
8: $sum\Omega$=$sum\Omega + 1/R_G[i, j]$;
9: **end if**
10: **end for**
11: **end for**
12: $\Omega_{glob} = sum\Omega/[n * (n-1)]$;

represents resistive matrix of G. Note that at line 2, line 3 and line 4, A_G, D_G and L_G indicate adjacency matrix, degree matrix and Laplacian matrix, respectively. At line 5, J is a square matrix and all of its elements are 1. Lines 6-8 present the formulations of $R_m(G)$. Moreover, the entry of $R_m(G)$, denoted by r_{ij}, can also be expressed as $r_{ij} = x_{ii} + x_{jj} - 2x_{ij}$, where $X = ||x_{ij}|| = (L + \frac{1}{n}J)^{-1}$. Refer to [39] for more details.

Algorithm 2 presents the calculation method of Kirchhoff index according to Eq. (15). *Kf* is closely related to the spectrum of the Laplacian matrix L_G (for more details see [10]). At line 2, $\mu List$ denotes a list of all the eigenvalues of Laplacian matrix L_G.

Algorithm 3 displays how to calculate average resistive path length L_r according to Eq. (16). At first, we compute resistive matrix $R_m(G)$ of G according to algorithm 1 (see line 2). Subsequently, L_r is obtained by $R_m(G)$, which is given at lines 3-10.

Algorithm 4 shows how to calculate resistive global efficiency Ω_{glob} according to Eq. (18). The execution of the method is similar to algorithm 3. At line 2, $R_m(G)$ is obtained. From line 3 to line 12, Ω_{glob} is computed by $R_m(G)$. Note that $R_m(G)[i, i] = 0$ for any i.

Algorithm 5 presents the method of local resistive efficiency Ω_{loc} according to Eqs. (19) and (20). Input is also

$$R_m[G_2''] = \begin{array}{c} \\ 0 \\ 3 \\ 4 \\ 5 \\ 6 \\ 7 \\ 8 \\ 1 \end{array} \begin{array}{c} \begin{array}{cccccccc} 0 & 3 & 4 & 5 & 6 & 7 & 8 & 1 \end{array} \\ \begin{pmatrix} 0 & 1 & 2 & 3 & +\infty & +\infty & +\infty & +\infty \\ 1 & 0 & 1 & 2 & +\infty & +\infty & +\infty & +\infty \\ 2 & 1 & 0 & 1 & +\infty & +\infty & +\infty & +\infty \\ 3 & 2 & 1 & 0 & +\infty & +\infty & +\infty & +\infty \\ +\infty & +\infty & +\infty & +\infty & 0 & 1 & 1.67 & 1.67 \\ +\infty & +\infty & +\infty & +\infty & 1 & 0 & 0.67 & 0.67 \\ +\infty & +\infty & +\infty & +\infty & 1.67 & 0.67 & 0 & 0.67 \\ +\infty & +\infty & +\infty & +\infty & 1.67 & 0.67 & 0.67 & 0 \end{pmatrix} \end{array}.$$

Algorithm 5 *Calculate*Ω_{loc}

Input: $G(V, E)$
Output: $\Omega_{loc}(v)$, $\Omega_{loc}(G)$

1: $n = |G(V, E)|$;
2: $\Omega_{loc}(G) = 0$;
3: **for** v in G **do**
4: $\Omega_{loc}(v) = 0$;
5: $v\_neighbors = Neighbors(v)$;
6: $v\_n\_len = Len(neighbors)$;
7: $G_v = Subgraph(v\_neighbors)$;
8: **if** $v\_n\_len == 1$ **then**
9: $\Omega_{loc}(v) = 0$;
10: continue;
11: **end if**
12: $cc\_list = ConnectedComponents(G_v)$;
13: $v\_sum = 0$;
14: **for** cc in cc_list **do**
15: $cc\_sum = \sum_{i \neq j \in cc} \frac{1}{r_{ij}}$;
16: $v\_sum = v\_sum + cc\_sum$;
17: **end for**
18: $\Omega_{loc}(v) = v\_sum/[(v\_n\_len) * (v\_n\_len - 1)]$;
19: $\Omega_{loc}(G) = \Omega_{loc}(G) + \Omega_{loc}(v)$;
20: **end for**
21: $\Omega_{loc}(G) = \Omega_{loc}(G)/n$;

Algorithm 6 *Calculate*D_r

Input: $G(V, E)$
Output: $D_r(v)$, $D_r(G)$

1: $n = |G(V, E)|$;
2: $R_m(G) = calculateR(G)$;
3: **for** v in G **do**
4: $v\_neighbors = Neighbors(v)$;
5: $deg = Degree(v, G)$;
6: **if** $deg == 1$ **then**
7: $D_r(v) = 0$;
8: continue;
9: **end if**
10: $sum = 0$;
11: $potential = [deg * (deg - 1)]/2$;
12: **for** u, w in $v\_neighbors$ **do**
13: $sum = sum + 1/R_m(G)[u, w]$;
14: **end for**
15: $sum = sum/potential$;
16: $D_r(v) = sum$;
17: $D_r(G) = D_r(G) + D_r(v)$;
18: **end for**
19: $D_r(G) = D_r(G)/n$;

a graph G. Two outputs, $\Omega_{loc}(v)$ and $\Omega_{loc}(G)$, denote local resistive efficiency of node v and that of graph G, respectively. At lines 5 and 6, $v\_neighbors$ indicates neighbors of v and v_n_len is its number. G_v is the induced subgraph of open neighborhood of node v at line 7. If v_n_len equals to 1, G_v is a trivial graph and $\Omega_{loc}(v) = 0$ (See lines 8-11). Otherwise, the set of connected components of G_v, denoted by cc_list at line 12, is computed. Usually, G_v is an unconnected graph. Therefore, at lines 14-17, $\Omega_{loc}(v)$ and $\Omega_{loc}(G)$ are obtained by enumerating each connected component of G_v.

Algorithm 6 computes loop coefficient D_r according to Eq. (24). Similarly, resistive matrix $R_m(G)$ of G is obtained at first at line 2. $v\_neighbors$ also represents the set of neighbors of v at line 4. If v has only one neighbor, $D_r(v) = 0$, which is displayed at lines 5-9. Otherwise, $D_r(v)$ is calculated through lines 10-16, where $R_G[u, w]$ indicates the resistive distance between node u and w.

V. EXPERIMENTAL RESULTS AND ANALYSIS

In this section, we assess the effectiveness of our descriptors on computer-generated and real-world networks, and make comparisons with baseline metrics. All the experiments are run on a PC equipped with a 2.7 GHz Intel Core i5-7200U CPU and 8.00G memory operating in the Microsoft windows 10 environment. Our codes are conducted relying upon python programming language. Especially, python packages, such as networkx, numpy and matplotlib, are utilized for modeling the networks, computation of data and visualization, respectively.

A. COMPUTER-GENERATED NETWORKS

In this section, we considered our proposed descriptors for three representative models of complex networks, the WS model [2], the ER model [3] and the BA model [1]. We calculate every descriptor's value for each classical network model. This experiment is conducted with network size $N = 1000$. As Tables 4-6 show, the values of all the descriptors in this work are given, for Small-world networks, ER random networks and Scale-free networks, respectively. Moreover, the values in terms of resistive distance are emphasized in bold.

1) Small-world networks
In this work, we construct small-world networks by Watts-Strogatz models. The initial graph is taken to be a one-dimensional lattice of $N = 1000$ nodes. It meets the periodic boundary conditions, i.e., each node is connected to its first $k = 4$ neighbors. The small-world network is created by rewiring each edge of the lattice at random with probability p. The transition from a regular lattice ($p = 0$) to random network ($p = 1$) can be obtained by varying p in a continuous way. Table 4 shows the values of structural quantities with p ranging progressively from 0 to 0.4.
As shown in Table 4, Kirchhoff index (Kf) and average resistive path length (L_r) decrease as p increases, which is consistent with Wiener index (W_r) and average path length (L). Overall, all the clustering coefficient descriptors, i.e., C_3, Ω_3, C_4, R, D, D_r, show similar actions with p. C_3 and C_4 decrease with increased p, so do R and D. Compared with C_3, Ω_3

TABLE 4. The values of global structural quantities for Small-world model networks with $N = 1000$, $k = 4$

p	$p=0$	$p=0.05$	$p=0.1$	$p=0.15$	$p=0.2$	$p=0.25$	$p=0.3$	$p=0.35$	$p=0.4$
Wr	62625000.0	5749503.0	4356787.0	3722952.0	3414384.0	3198683.0	3170978.0	2995138.0	2894453.0
Kf	**16756053.0**	**980659.0**	**692470.0**	**692470.0**	**513145.0**	**485477.0**	**470996.0**	**453559.0**	**430107.0**
L	125.3754	11.5105	8.7223	7.4534	6.8356	6.4038	6.3483	5.9963	5.7947
L_r	**33.5457**	**1.9633**	**1.3863**	**1.1511**	**1.0273**	**0.9719**	**0.9429**	**0.908**	**0.8611**
E_{glob}	0.0244	0.1018	0.1293	0.1484	0.1602	0.17	0.1712	0.1805	0.186
Ω_{glob}	**0.0648**	**0.5362**	**0.754**	**0.9039**	**1.0084**	**1.0706**	**1.0996**	**1.1534**	**1.2095**
E_{loc}	0.7222	0.5934	0.4896	0.3879	0.3184	0.252	0.2334	0.1687	0.1192
Ω_{loc}	**0.7222**	**0.5934**	**0.4896**	**0.3879**	**0.3184**	**0.252**	**0.2334**	**0.1687**	**0.1192**
$E_{loc'}$	**0.85**	**0.8292**	**0.8121**	**0.7936**	**0.7814**	**0.7682**	**0.7644**	**0.751**	**0.7401**
$\Omega_{loc'}$	**1.5497**	**1.4105**	**1.2955**	**1.1782**	**1.0993**	**1.0209**	**0.9967**	**0.9185**	**0.8596**
SC	2.0094	1.9512	1.9004	1.8404	1.8041	1.7693	1.7484	1.7066	1.6686
C_3	0.5	0.4295	0.3703	0.3066	0.2613	0.2112	0.2018	0.1498	0.1083
Ω_3	**0.241**	**0.2013**	**0.1715**	**0.1416**	**0.1187**	**0.0959**	**0.0913**	**0.0677**	**0.0478**
C_4	0.1481	0.1127	0.0836	0.0661	0.0457	0.0363	0.0308	0.0231	0.0125
R	0.2833	0.2582	0.2362	0.2198	0.2008	0.189	0.1854	0.1709	0.1582
D	0.7222	0.6407	0.5681	0.5054	0.4437	0.3978	0.3851	0.3312	0.2854
D_r	**1.6426**	**1.6449**	**1.6326**	**1.6167**	**1.6144**	**1.6035**	**1.6044**	**1.5953**	**1.591**

TABLE 5. The values of global structural quantities for E-R model networks with 1000 nodes.

p	$p=0.025$	$p=0.05$	$p=0.075$	$p=0.1$	$p=0.125$	$p=0.15$	$p=0.175$	$p=0.2$
Wr	1246066	1012174	962992	949349	936499	923723	911855	898685
Kf	**43356**	**20702**	**13609**	**10237**	**8099**	**6706**	**5783**	**5015**
L	2.4946	2.0264	1.9279	1.9006	1.8749	1.8493	1.8255	1.7992
L_r	**0.0868**	**0.0414**	**0.0272**	**0.0205**	**0.0162**	**0.0134**	**0.0116**	**0.01**
E_{glob}	0.4259	0.5123	0.5371	0.5497	0.5626	0.5754	0.5872	0.6004
Ω_{glob}	**11.7819**	**24.3779**	**36.9535**	**49.0375**	**61.9008**	**74.7083**	**86.5957**	**99.8116**
E_{loc}	0.0361	0.2539	0.4222	0.4926	0.5414	0.5705	0.5866	0.6003
Ω_{loc}	**0.0366**	**0.5284**	**2.1129**	**4.265**	**7.1549**	**10.6958**	**14.5922**	**19.5381**
$E_{loc'}$	0.5515	0.5439	0.55	0.559	0.5696	0.5809	0.592	0.6044
$\Omega_{loc'}$	**0.7149**	**1.373**	**2.8325**	**4.9288**	**7.8016**	**11.3396**	**15.2387**	**20.1892**
SC	2.10e+19	1.66e+19	1.27e+30	3.71e+40	4.77e+51	5.83e+62	1.20e+73	3.06e+84
C_3	0.0252	0.05	0.0755	0.0998	0.1252	0.1506	0.1746	0.2008
Ω_3	**0.002**	**0.002**	**0.002**	**0.002**	**0.002**	**0.002**	**0.002**	**0.002**
C_4	0.001	0.0011	0.0012	0.0.0012	0.0013	0.0014	0.0015	0.0016
R	0.2259	0.2503	0.2561	0.2583	0.2604	0.2626	0.2646	0.2667
D	0.4252	0.5122	0.5372	0.5499	0.5626	0.5753	0.5873	0.6004
D_r	**12.29**	**24.88**	**37.45**	**49.52**	**62.35**	**75.15**	**87.04**	**100.22**

TABLE 6. The values of global structural quantities for scale-free model networks with 1000 nodes.

m	$m=1$	$m=2$	$m=3$	$m=4$	$m=5$	$m=6$
Wr	3191651.0	2054321.0	1736308.0	1567454.0	1481918.0	1412634.0
Kf	**3191651.0**	**488722.0**	**283127.0**	**200405.0**	**153874.0**	**124875.0**
L	6.3897	4.1128	3.4761	3.138	2.9668	2.8281
L_r	**6.3897**	**0.9784**	**0.5668**	**0.4012**	**0.3081**	**0.25**
E_{glob}	0.1782	0.259	0.3049	0.3361	0.3544	0.3714
Ω_{glob}	**0.1782**	**1.1216**	**1.9467**	**2.7526**	**3.597**	**4.4143**
E_{loc}	0.0	0.0272	0.0353	0.0483	0.0508	0.0684
Ω_{loc}	**0.0**	**0.0272**	**0.0359**	**0.0507**	**0.0558**	**0.0793**
$E_{loc'}$	**0.92**	**0.7659**	**0.6957**	**0.6605**	**0.6346**	**0.6201**
$\Omega_{loc'}$	**0.92**	**0.7865**	**0.7413**	**0.7393**	**0.7319**	**0.7631**
SC	26.5633	46.7249	2161.3778	72471.6463	625879.296	17777606.290
C_3	0.0	0.0268	0.0316	0.0399	0.0392	0.0473
Ω_3	**0.0**	**0.006**	**0.0045**	**0.0048**	**0.0041**	**0.004**
C_4	0.0	0.0037	0.0026	0.0022	0.0021	0.002
R	0.0	0.1835	0.2019	0.2141	0.2191	0.2249
D	0.0	0.3087	0.3574	0.3935	0.408	0.4268
D_r	**0.1685**	**2.5137**	**3.8584**	**5.2622**	**6.4824**	**7.855**

displays a consistent performance, i.e., 0.241, 0.2013, 0.1715, 0.1416, 0.1187, 0.0959, 0.0913, 0.0677, 0.0478 with increased p. D_r doesn't have a perfect performance, but it overall decreases when p increases significantly.

To compare L and L_r for the WS network model, Figure 3 (a) illustrates the data normalized by the $L(0)$ and $L_r(0)$, which are 125.3754 and 3385, respectively. Figure 3 shows the plot of the normalized average shortest path length $L(p)/L(0)$, the normalized

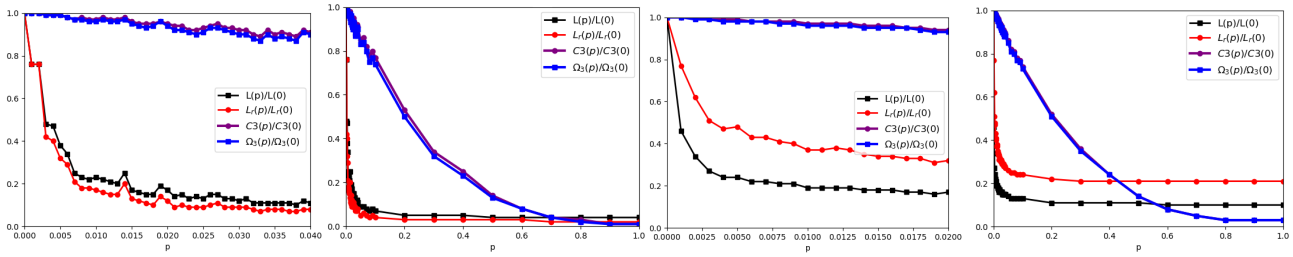

(a) N=4,$p \leqslant 0.04$ (b) N=4,$p \leqslant 1$ (c) N=20,$p \leqslant 0.04$ (d) N=20,$p \leqslant 1$

FIGURE 3. The average shortest path length $L(p)$, the average resistive path length $L_r(p)$, the ordinary clustering coefficient C_3 and the resistive clustering coefficient Ω_3 for the WS network model. The data is normalized by the $L(p)(0)$, $L_r(p)(0)$, $C_3(0)$ and $\Omega_3(0)$. The network size $N = 1000$, $m = 4$ for (a) and (b), $m = 20$ for (c) and (d).

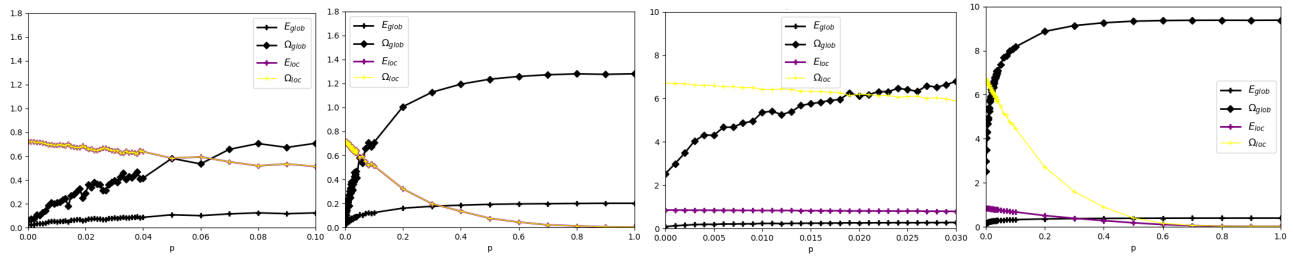

(a) N=4,$p \leqslant 0.04$ (b) N=4,$p \leqslant 1$ (c) N=20,$p \leqslant 0.04$ (d) N=20,$p \leqslant 1$

FIGURE 4. The ordinary global efficiency E_{glob}, local efficiency E_{loc} and their corresponding resistive efficiency Ω_{glob} and Ω_{loc} for the WS network model. The network size $N = 1000$, $m = 4$ for (a) and (b), $m = 20$ for (c) and (d).

the average resistive path length $L_r(p)/L_r(0)$, the normalized ordinary clustering coefficient $C_3(p)/C_3(0)$ and the normalized resistive clustering coefficient $\Omega_3(p)/\Omega_3(0)$ as functions of the rewiring probability p. The seminal work of Watts and Strogatz [2] uses the combination of high clustering coefficient and short average path length to define the characteristics of small-world networks. They found that, when rewiring probability p <0.01, average path length L (black line) has a rapid drop, whereas the clustering coefficient C_3 (blue line) stays almost constant. Interestingly, the resistive clustering coefficient Ω_3 (purple line) also stays nearly unchanged when p <0.01 (see Figure 3 (a)) and drops to 0 when $p = 1$ (see Figure 3 (b)). Likewise, rewiring just a few edges ($p < 0.01$) also can lead to a dramatic reduction in the average resistive path length L_r (red line).

Figure 4 shows the plot of the ordinary global efficiency E_{glob}, local efficiency E_{loc} and their corresponding resistive efficiency Ω_{glob} and Ω_{loc} as functions of the rewiring probability p. According to the work of Latora and Marchiori [9], small-world networks can be seen as systems that have high E_{glob} and high E_{loc}. A regular lattice with N=1000 and k=4 (20) is rewired with probability p. The introduction of only a few rewired edges (p ranging from 0 to 0.01) result in a dramatic increase of E_{glob} and the a very little decrease of E_{loc}. Luckily, Ω_{glob} and Ω_{loc} also display the same features (see Figure 4).

2) ER random networks Erdös-Rényi model is also known as $G_{n,p}$ model. The algorithm chooses each of the $[n(n-1)]/2$ possible edges with probability p. Table 5 shows the values of structural quantities for the ER networks with network size N=1000 and p ranging progressively from 0.05 to 0.2. As p increases, W_r (resp., Kf), L (resp., L_r) decrease, while E_{glob} (resp., Ω_{glob}), E_{loc} (resp., Ω_{loc}) increase, R and D (resp., D_r) increase, respectively. That is to say, resistive descriptors, Kf, L_r, Ω_{glob}, Ω_{loc}, D_r, have similar characteristics with classic descriptors in ER model networks. It is well known that C_3 is equal to its probability for edge creation in an ER network. While, Ω_3 is a constant in ER networks when network size is given.
3) Scale-free networks Scale-free networks are constructed by BA model, which refers to Barabási-Albert preferential attachment model. A graph of N nodes is expanded by attaching new nodes each with m edges that are preferentially attached to existing nodes with high degree. Table 6 shows the values of structural quantities for the BA networks with $N = 1000$ and m ranging from 1 to 6. As m increases, W_r (resp., Kf), L (resp., L_r) decrease, E_{glob} (resp., Ω_{glob}), E_{loc} (resp., Ω_{loc}) increase, R and D (resp., D_r) increase, respectively. That is, resistive descriptors, Kf, L_r, Ω_{glob}, Ω_{loc}, D_r, show similar characteristics with classic descriptors in BA model networks. However, Ω_3 displays different results from C_3 in BA model networks.

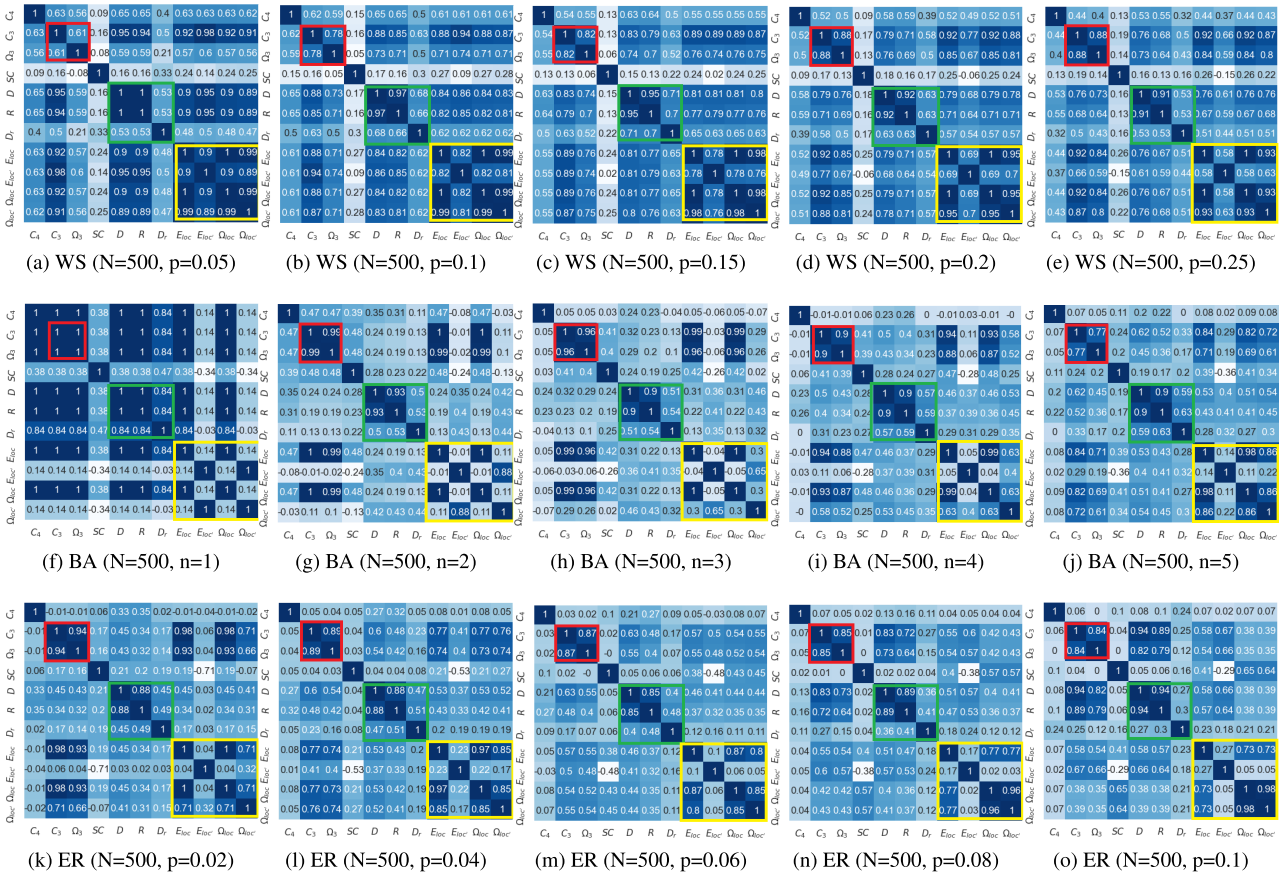

(a) WS (N=500, p=0.05) (b) WS (N=500, p=0.1) (c) WS (N=500, p=0.15) (d) WS (N=500, p=0.2) (e) WS (N=500, p=0.25)

(f) BA (N=500, n=1) (g) BA (N=500, n=2) (h) BA (N=500, n=3) (i) BA (N=500, n=4) (j) BA (N=500, n=5)

(k) ER (N=500, p=0.02) (l) ER (N=500, p=0.04) (m) ER (N=500, p=0.06) (n) ER (N=500, p=0.08) (o) ER (N=500, p=0.1)

FIGURE 5. The Kendall's Tau correlation matrices, between the ranking scores of different structural descriptors, are shown for the WS, ER and BA networks of $N = 500$, which are under different parameters.

B. THE KENDALL's TAU FOR WS, ER AND BA MODELS

To evaluate the performance of the proposed structural descriptors, we investigate the Kendall's Tau (τ) between the ranking scores of different methods. Higher τ suggests better performance. Given two ranking scores of X and Y, if τ is more closer to 1, it means that X and Y are more highly correlated. Figure 5 shows the Kendall's Tau correlation cofficient matrices between the ranking scores given by eleven local structural properties, i.e., $C_4, C_3, \Omega_3, SC, D, R, D_r, E_{loc}, E_{loc'}$, $\Omega_{loc}, \Omega_{loc'}$. Three classic networks models, i.e., WS, ER and BA, are considered with network size $N = 500$. For WS networks, $k = 5$, and p ranging from 0.05 to 0.25, i.e., 0.05, 0.1, 0.15, 0.2, 0.25. For ER networks, p, probability for edge creation, varies from 0.02 to 0.1. For BA networks, the values of m, number of edges attached from a new node to existing nodes, are 1, 2, 3, 4, 5. We classify all the structural properties into three comparative groups, i.e., C_3, and Ω_3 for the first group, D, R, and D_r for the second group, E_{loc}, $E_{loc'}$, Ω_{loc}, and $\Omega_{loc'}$ for the last group. As shown in Figure 5, the values, bordered in red, green, and yellow, correspond to the matrix of the first, second and third group, respectively. The following discussions suggest more details for each group.

First, we make an assumption that the Kendall's Tau between C_3 and Ω_3 is inversely related to the standard average clustering coefficient (C_3) of the target network. A network with a high average clustering coefficient indicates that the network is more clustered. That is to say, there are more paths for any pair of nodes. However, in general, for any two nodes, less paths can lead to a observation that the resistive distance between them is more close to 1. In terms of a node, resistive clustering coefficient Ω_3 is more close to typical clustering coefficient C_3. As is well known, average clustering coefficient of small-world networks decreases with the increasing rewiring probability, while that of ER random networks increases with the probability for edge creation. As can be seen from Figure 5, the matrices with red borders illustrate the Kendall's τ between C_3 and Ω_3. In WS model, shown from (a) to (e), $\tau = 0.61, 0.78, 0.82, 0.88, 0.88$, when $p = 0.05, 0.1, 0.15, 0.2, 0.25$, respectively. Clearly, τ grows with the increased p. In BA model, shown from (f) to (j), $\tau = 1, 0.99, 0.96, 0.9, 0.77$, when $n = 1, 2, 3, 4, 5$. Obviously, τ decreases when n increases. In ER model, shown from (k) to (o), $\tau = 0.94, 0.89, 0.87, 0.85, 0.84$, when $p = 0.02, 0.04, 0.06, 0.08, 0.1$. Of course, τ increases when the probability for edge creation increases progressively.

Second, we turn to the discussion of D, R and D_r. D is close to R. As D considers the length of shortest path, while R applies that of the smallest cycle. However, regardless of

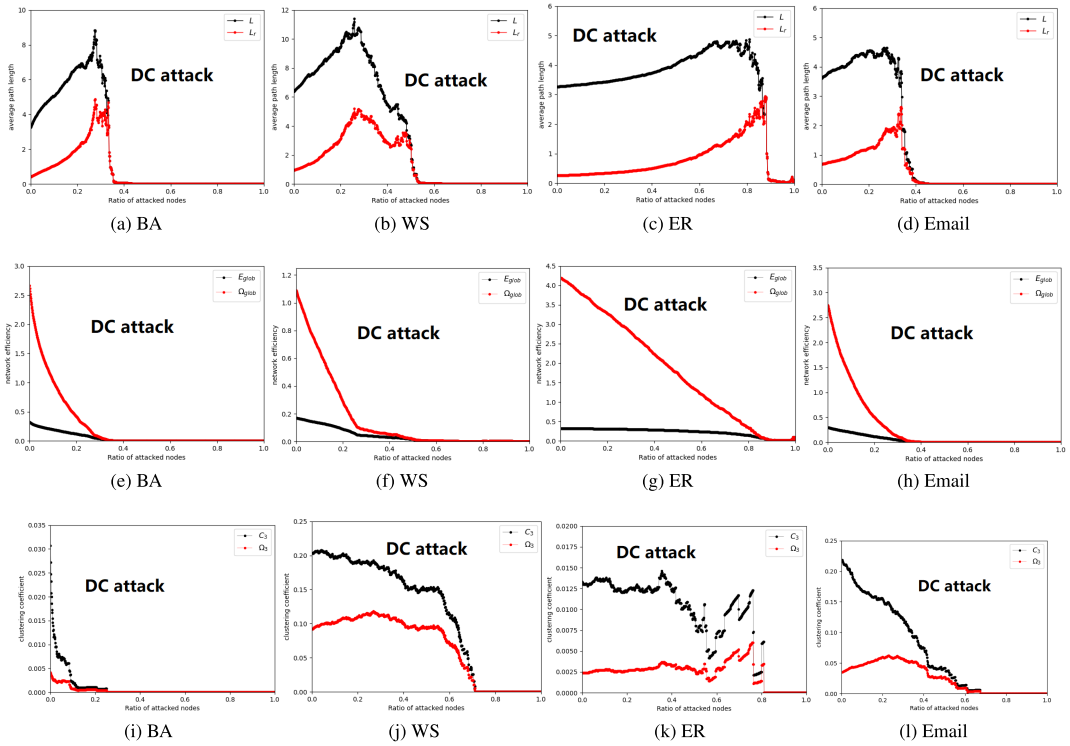

FIGURE 6. Comparisons of different invulnerability metrics under Degree Centrality attack.

TABLE 7. The values of structural quantities for eight real networks.

structural descriptors	BioCEGN	NS	USAir	Karate	Dolphin	Football	Jazz	Email
$\|V\|$	2215	379	332	34	62	115	198	1133
$\|E\|$	53680	914	2126	78	159	613	2742	5451
Wr	6616502	432785	150449	1351	6348	16441	43590	2312469
Kf	**576643**	**148258**	**3482466**	**470**	**1864**	**1509**	**3992**	**436814**
L	2.6984	6.0419	2.7381	2.4082	3.357	2.5082	2.235	3.606
L_r	**0.2352**	**2.0697**	**63.3798**	**0.8383**	**0.9859**	**0.2302**	**0.2047**	**0.6812**
SC	2.8e+38	125.2	2.4e+15	30.6	33.2	704.4	1.2e+15	928566.9
λ	122.6	4.8299	0.1989	3.4218	3.5028	6.5573	34.7391	13.7414
E_{glob}	0.401	0.2032	0.4059	0.492	0.3792	0.4504	0.5132	0.2999
Ω_{glob}	**20.6353**	**0.6056**	**0.1416**	**1.4341**	**1.4335**	**4.3883**	**10.4518**	**2.7751**
E_{loc}	0.393	0.7842	0.7092	0.6451	0.3399	0.5121	0.7808	0.3122
Ω_{loc}	**3.9678**	**1.3787**	**0.2115**	**0.7743**	**0.5101**	**1.5095**	**7.2462**	**0.6242**
$E_{loc'}$	**0.6684**	**0.9305**	**0.9172**	**0.8709**	**0.8087**	**0.7534**	**0.8393**	**0.7634**
$\Omega_{loc'}$	**5.0714**	**2.0336**	**0.2375**	**1.4806**	**1.3565**	**2.3536**	**7.9861**	**1.4519**
C_3	0.1843	0.7412	0.6252	0.5706	0.259	0.4032	0.6175	0.2202
Ω_3	**0.0051**	**0.2921**	**6.6977**	**0.1566**	**0.0766**	**0.0717**	**0.0462**	**0.0345**
C_4	0.0128	0.4047	0.1897	0.2882	0.1075	0.0499	0.0666	0.0146
R	0.2478	0.2809	0.2566	0.2852	0.2113	0.2696	0.2927	0.2102
D	0.554	0.8027	0.7207	0.7556	0.491	0.6557	0.7896	0.4727
D_r	**49.839**	**2.5193**	**0.9436**	**3.4684**	**2.2205**	**4.9888**	**15.7828**	**5.7266**

each model, the correlation values, between D_r and D (R), has no functional relation to its parameter.

Third, the last group, i.e., E_{loc}, $E_{loc'}$, Ω_{loc}, and $\Omega_{loc'}$, displays some interesting results. Comparatively, we have more concerns about the values between E_{loc} and Ω_{loc}. Excitedly, in WS and BA models, the Kendall's τ, in terms of any network's parameters, are close to 1 or equal to 1. In addition, in WS and BA models, under the condition of network's

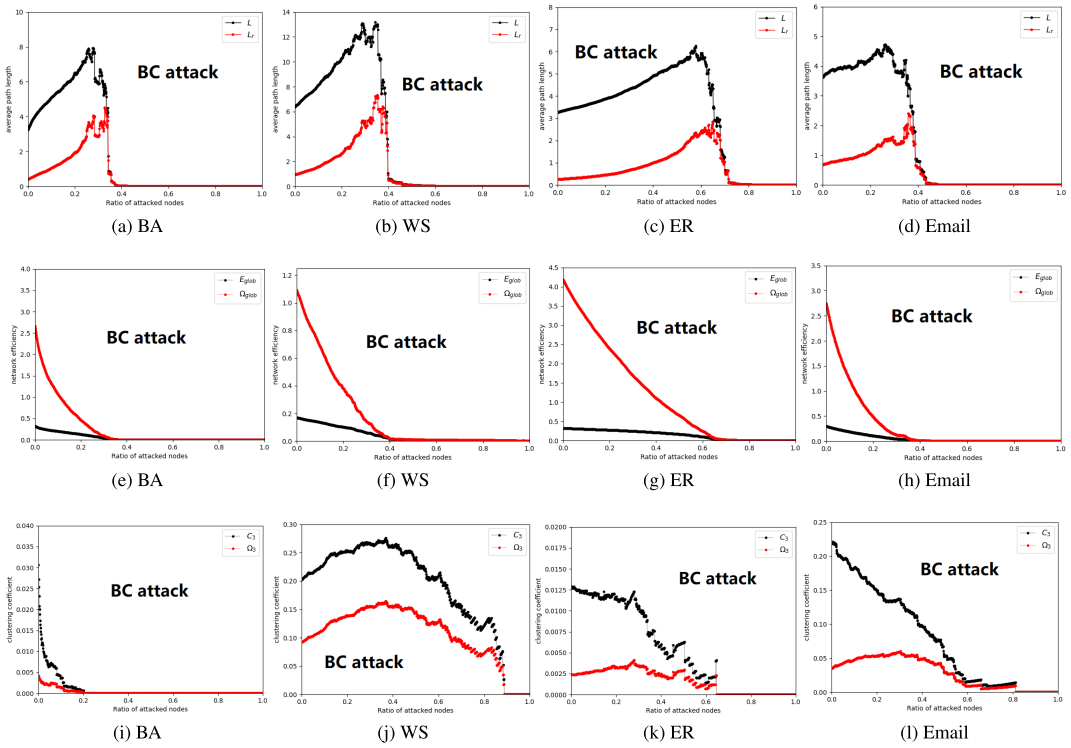

FIGURE 7. Comparisons of different invulnerability metrics under Betweenness Centrality attack.

parameters that we set, for each node v of the network, it is possible that $E_{loc}(v) = \Omega_{loc}(v)$. Refer to Table 4 and 6 for the comparisons between $E_{loc}(v)$ and $\Omega_{loc}(v)$. As described in Section III, if G_v is a tree, for any node i, j in G_v, $r_{ij} = d_{ij}$, where r_{ij} and d_{ij} are resistive distance and shortest path distance, respectively. Therefore, if G_v is a tree, $E_{loc}(v) = \Omega_{loc}(v)$.

Besides, in ER model, $\tau = 1, 0.97, 0.87, 0.77, 0.73$, when $p = 0.02, 0.04, 0.06, 0.08, 0.1$, respectively. It indicates an inverse association between τ and p. Moreover, p equals to C_3 in ER networks. In other words, τ between E_{loc} and Ω_{loc}, in terms of ER random networks, is inverse to the ordinary clustering coefficient (C_3). For more details for this group, see the matrices bordered in yellow, shown in Figure 5.

The experiments are carried on eight real networks from disparate fields, including one transportation network (USAir), one biological network (bio-CE-GN), one communication network (Email), two collaboration networks (NS and Jazz), three social networks (Karate, Dolphin and Football). In brief, USAir [45] is the US air transportation network. CE-GN [47] is a biological network and its links are inferred by gene neighbourhoods of bacterial and archaeal orthologs. Email [44] is a network of E-mail interchanges between members of the Rovira i Virgili University. NS [46] is a co-authorship network of scientists working on network science. Jazz [43] is a collaboration network between jazz musicians consisting of 198 nodes and 2,742 edges. Karate [40] is an undirected social network of friendships between 34 club members of a karate club at a US university in the 1970s; Dolphin [41] is an undirected social network of frequent associations between 62 dolphins during a community living off Doubtful Sound, New Zealand; Football [42] is an undirected social network of American football games between Division IA colleges during regular season Fall 2000. The values of structural quantities for eight real networks are shown in Table 7.

C. INTENTIONAL ATTACKS BASED ON DC AND BC

In this section, experiments are conducted for the BA ($N = 1000$, $n = 4$), WS ($N = 1000$, $m = 4$, $p = 0.3$), ER ($N = 1000$, $p = 0.01$) and real networks under Degree Centrality attack and Betweenness Centrality attack. Email network is selected as an example for real networks. Different invulnerability metrics, including average path length (L and L_r), network efficiency (E_{glob} and Ω_{glob}), clustering coefficient (C_3 and Ω_3) are considered. The results under *DC* attack and *BC* attack are shown in Figure 6 and Figure 7, respectively. Clearly, the curve of each novel vulnerability metric is similar with that of the baseline method. Moreover, we compare the running time for calculating four global structural metrics (L, L_r, E_{glob}, Ω_{glob}) in different network, as shown in Table 8. Obviously, the resistive descriptors have better performance. Resistive metrics are based on matrix calculation, while the shortest path metrics are based on graph searching algorithms. From this section's results, matrix

TABLE 8. Comparisons of running time of four global structural quantities in different network. Experiments are conducted for the BA ($N = 1000$, $n = 4$), WS ($N = 1000$, $m = 4$, $p = 0.3$), ER ($N = 1000$, $p = 0.01$).

structural descriptors	BA	WS	ER	Email
L	4.648s	4.357s	6.486s	6.391s
L_r	**1.054s**	**1.187s**	**1.421s**	**1.328s**
E_{glob}	4.750s	3.626s	5.130s	6.391s
Ω_{glob}	**1.391s**	**1.392s**	**1.39s**	**1.876s**

calculation are more efficient than graph searching algorithms. In other words, global metrics based on resistive distance are more efficient in the networks with small and medium size.

VI. CONCLUSION

In this work, analogous to classical statistical descriptors, novel resistive descriptors, including Kirchhoff index (Kf), average path length (L_r), clustering coefficient (Ω_3), loop coefficient (D_r), global efficiency (Ω_{glob}) and local efficiency (Ω_{loc}) are suggested. We investigate all the resistive descriptors on classical WS, BA and ER models. Interestingly, Ω_3 and L_r (resp., Ω_{glob} and Ω_{loc}) could be used to characterize the features of small-world networks. Besides, L_r, Ω_3 and Ω_{glob} are considered to measure network invulnerability based on DC and BC attack. Experiments are conducted on networks with small and medium size. The results show that, in terms of running time, resistive distance depending on matrix calculation is more efficient than the shortest-path distance mainly based on the searching algorithms. In the future, we will explore the potential use of the proposed structure descriptors in other issues of complex networks including community detection, link prediction, privacy preservation, etc.

REFERENCES

[1] A.-L. Barabási and R. Albert, "Emergence of scaling in random networks," *Science*, vol. 286, no. 5439, pp. 509–512, Oct. 1999.
[2] D. J. Watts and S. H. Strogatz, "Collective dynamics of 'small-world' networks," *Nature*, vol. 393, no. 6684, pp. 440–442, 1998.
[3] V. Batagelj and U. Brandes, "Efficient generation of large random networks," *Phys. Rev. E, Stat. Phys. Plasmas Fluids Relat. Interdiscip. Top.*, vol. 71, no. 3, Mar. 2005, Art. no. 036113.
[4] Y. Qian, B. Wang Y. Xue, J. Zeng, and N. Wang, "A simulation of the cascading failure of a complex network model by considering the characteristics of road traffic conditions," *Nonlinear Dyn.*, vol. 80, nos. 1–2, pp. 413–420, 2015.
[5] J. Zhang, Y. Dai, K. Zou, B. Song, and Z. Zhang, "Vulnerability analysis of the U.S. power grid based on local load-redistribution," *Saf. Sci.*, vol. 80, pp. 156–162, Dec. 2015.
[6] Y. Zeng and R. Xiao, "Modelling of cluster supply network with cascading failure spread and its vulnerability analysis," *Int. J. Prod. Res.*, vol. 52, no. 23, pp. 6938–6953, May 2014.
[7] R. Albert, H. Jeong, and A.-L. Barabási, "Error and attack tolerance of complex networks," *Nature*, vol. 406, no. 6794, pp. 378–382, Jul. 2000.
[8] M. Jalili, "Error and attack tolerance of small-worldness in complex networks," *J. Informetrics*, vol. 5, no. 3, pp. 422–430, Jul. 2011.
[9] V. Latora and M. Marchiori, "Efficient behavior of small-world networks," *Phys. Rev. Lett.*, vol. 87, no. 19, pp. 198701–198704, Oct. 2001.
[10] D. J. Klein and M. Randić, "Resistance distance," *J. Math. Chem.*, vol. 12, no. 1, pp. 81–95, Dec. 1993.
[11] K. Stephenson and M. Zelen, "Rethinking centrality: Methods and examples," *Soc. Netw.*, vol. 11, no. 1, pp. 1–37, 1989.
[12] W. J. Xiao and I. Gutman, "Resistance distance and Laplacian spectrum," *Theor. Chem. Accounts*, vol. 110, no. 4, pp. 284–289, Nov. 2003.
[13] R. Bapat, I. Gutman, and W. Xiao, "A simple method for computing resistance distance," *Zeitschrift Naturforschung A*, vol. 58, pp. 494–498, Oct. 2003.
[14] H. Chen and F. Zhang, "Resistance distance and the normalized Laplacian spectrum," *Discrete Appl. Math.*, vol. 155, no. 5, pp. 654–661, Mar. 2007.
[15] Y. Yang and Y. Yu, "Resistance distances and Kirchhoff indices under graph operations," *IEEE Access*, vol. 8, pp. 95650–95656, 2020.
[16] L. Zhang and J.-B. Liu, "Theoretical and computational methods to resistance distances in novel graphs operations," *IEEE Access*, vol. 7, pp. 107908–107916, 2019.
[17] W. Wang, T. Ma, and J.-B. Liu, "Resistance distance and Kirchhoff index of Q-double join graphs," *IEEE Access*, vol. 7, pp. 102313–102320, 2019.
[18] M. S. Sardar, J.-B. Liu, I. Siddique, and M. M. M. Jaradat, "A novel and efficient method for computing the resistance distance," *IEEE Access*, vol. 9, pp. 107104–107110, 2021.
[19] B. Lu, C.-Y. Liu, and Y.-H. Wang, "Discovery of community structure in complex networks based on resistance distance and center nodes," *J. Comput. Inform. Syst.*, vol. 8, no. 23, pp. 9807–9814, Dec. 2012.
[20] T. Zhang and C. Bu, "Detecting community structure in complex networks via resistance distance," *Phys. A, Stat. Mech. Appl.*, vol. 526, Jul. 2019, Art. no. 120782.
[21] W. Li, H. Zhu, S. Li, H. Wang, H. Dai, C. Wang, and Q. Jin, "Evolutionary community discovery in dynamic social networks via resistance distance," *Expert Syst. Appl.*, vol. 171, Jun. 2021, Art. no. 114536.
[22] P. Lu, Z. Yu, and Y. Guo, "A novel algorithm for community detection based on resistance distance and similarity," *Modern Phys. Lett. B*, vol. 35, no. 9, Mar. 2021, Art. no. 2150164.
[23] W. Lin, M. Li, S. Zhou, J. Liu, G. Chen, and Q. Zhou, "Phase transition in spectral clustering based on resistance matrix," *Phys. A, Stat. Mech. Appl.*, vol. 566, Mar. 2021, Art. no. 125598.
[24] U. Brandes and D. Fleischer, "Centrality measures based on current flow," in *Proc. STACS*, 2005, pp. 533–544.
[25] E. Bozzo and M. Franceschet, "Resistance distance, closeness, and betweenness," *Social Netw.*, vol. 35, no. 3, pp. 460–469, Jul. 2013.
[26] C. Gutiérrez, J. Gancio, C. Cabeza, and N. Rubido, "Finding the resistance distance and eigenvector centrality from the network's eigenvalues," *Phys. A, Stat. Mech. Appl.*, vol. 569, May 2021, Art. no. 125751.
[27] D. Liben-Nowell and J. Kleinberg, "The link-prediction problem for social networks," *J. Amer. Soc. Inf. Sci. Technol.*, vol. 58, pp. 1019–1031, May 2007.
[28] W. Ellens, "Effective resistance and other graph measures for network robustness," M.S. thesis, Dept. Appl. Math., Math. Inst., Univ. Leiden, Leiden, The, Netherlands, Apr. 2011.
[29] A. Tizghadam and A. Leon-Garcia, "Betweenness centrality and resistance distance in communication networks," *IEEE Netw.*, vol. 24, no. 6, pp. 10–16, Nov. 2010.
[30] M. Tyloo, T. Coletta, and P. Jacquod, "Robustness of synchrony in complex networks and generalized Kirchhoff indices," *Phys. Rev. Lett.*, vol. 120, no. 8, Feb. 2018, Art. no. 084101.
[31] M. Tyloo and P. Jacquod, "Global robustness versus local vulnerabilities in complex synchronous networks," *Phys. Rev. E, Stat. Phys. Plasmas Fluids Relat. Interdiscip. Top.*, vol. 100, no. 3, Sep. 2019, Art. no. 032303.
[32] A. K. Chandra, P. Raghavan, W. L. Ruzzo, R. Smolensky, and P. Tiwari, "The electrical resistance of a graph captures its commute and cover times," *Comput. Complex.*, vol. 6, no. 4, pp. 312–340, 1996.
[33] H. Wiener, "Structure determination of paraffin boiling points," *J. Amer. Chem. Soc.*, vol. 69, pp. 17–20, Jan. 1947.
[34] P. G. Lind, M. C. González, and H. J. Herrmann, "Cycles and clustering in bipartite networks," *Phys. Rev. E, Stat. Phys. Plasmas Fluids Relat. Interdiscip. Top.*, vol. 72, no. 5, Nov. 2005, Art. no. 056127.
[35] E. Estrada and J. A. Rodríguez-Velázquez, "Subgraph centrality in complex networks," *Phys. Rev. E, Stat. Phys. Plasmas Fluids Relat. Interdiscip. Top.*, vol. 71, no. 5, May 2005, Art. no. 056103.
[36] J. Wu, M. Barahona, Y.-J. Tan, and H.-Z. Deng, "Spectral measure of structural robustness in complex networks," *IEEE Trans. Syst., Man, Cybern. A, Syst., Humans*, vol. 41, no. 6, pp. 1244–1252, Nov. 2011.

[37] H.-J. Kim and J. M. Kim, "Cyclic topology in complex networks," *Phys. Rev. E, Stat. Phys. Plasmas Fluids Relat. Interdiscip. Top.*, vol. 72, no. 3, Sep. 2005, Art. no. 036109.
[38] I. Vragović and E. Louis, "Network community structure and loop coefficient method," *Phys. Rev. E, Stat. Phys. Plasmas Fluids Relat. Interdiscip. Top.*, vol. 74, Jul. 2006, Art. no. 016105.
[39] D. Babić, D. J. Klein, I. Lukovits, S. Nikolić, and N. Trinajstić, "Resistance-distance matrix: A computational algorithm and its application," *Int. J. Quant. Chem.*, vol. 90, no. 1, pp. 166–176, 2002.
[40] W. W. Zachary, "An information flow model for conflict and fission in small groups," *J. Anthropol. Res.*, vol. 33, no. 4, pp. 452–473, 1977.
[41] D. Lusseau, K. Schneider, O. J. Boisseau, P. Haase, E. Slooten, and S. M. Dawson, "The bottlenose dolphin community of doubtful sound features a large proportion of long-lasting associations," *Behav. Ecol. SocioBiol.*, vol. 54, no. 4, pp. 396–405, Sep. 2003.
[42] M. Girvan and M. E. J. Newman, "Community structure in social and biological networks," *Proc. Nat. Acad. Sci. USA*, vol. 99, no. 12, pp. 7821–7826, Apr. 2002.
[43] P. M. Gleiser and L. Danon, "Gleiser community structure in jazz," *Adv. Complex Syst.*, vol. 6, no. 4, pp. 565–573, Dec. 2003.
[44] R. Guimerà, L. Danon, A. Díaz-Guilera, F. Giralt, and A. Arenas, "Self-similar community structure in a network of human interactions," *Phys. Rev. E, Stat. Phys. Plasmas Fluids Relat. Interdiscip. Top.*, vol. 68, no. 6, Dec. 2003, Art. no. 065103.
[45] V. Batageli and A. Mrvar. *Pajek Datasets*. Accessed: 2007. [Online]. Available: http://vlado.fmf.uni-lj.si/pub/networks/data/
[46] M. E. J. Newman, "Finding community structure in networks using the eigenvectors of matrices," *Phys. Rev. E, Stat. Phys. Plasmas Fluids Relat. Interdiscip. Top.*, vol. 74, no. 3, Sep. 2006, Art. no. 036104.
[47] R. A. Rossi and N. K. Ahmed. *The Network Data Repository With Interactive Graph Analytics and Visualization*. Accessed: 2015. [Online]. Available: http://networkrepository.com/

MIN LI received the B.S. degree in computer science and technology and the M.S. degree in computer application technology from Xidian University, Xi'an, China, in 2008 and 2011, respectively. She is currently pursuing the Ph.D. degree with the College of Computer and Cyber Security, Fujian Normal University. She is also a Lecturer at the Concord University College, Fujian Normal University. Her research interests include graph theory, network science, data mining, and fault diagnosis.

SHUMING ZHOU received the Ph.D. degree in mathematics from Xiamen University, China, in June 2005. In 2005, he joined the School of Mathematics and Statistics, Fujian Normal University, where he is currently a Professor and a Ph.D. Supervisor. He was a Visiting Scholar at the University of Science and Technology of China, from September 2010 to July 2011. He has published over 80 technical papers in international journals, such as IEEE TRANSACTIONS ON COMPUTERS, IEEE TRANSACTIONS ON PARALLEL AND DISTRIBUTED SYSTEMS, IEEE TRANSACTIONS ON RELIABILITY, *INS*, IEEE TRANSACTIONS ON CIRCUITS AND SYSTEMS—I: REGULAR PAPERS, *JPDC*, *DAM*, *Physica A: Statistical Mechanics and its Applications*, and *PLA* on these topics, since 2005. His research interests include algorithmic graph theory, combinatorial optimization, fault diagnosis, network science, social networks, and big data processing. He received the Distinguishing Paper Award from the 3rd International Conference on Science of Cyber Security (Sci Sec 2021) and the First Prize of the Excellent Paper Award from the Fujian Association for Science and Technology, in 2016.

GAOLIN CHEN received the B.S. and M.S. degrees from the School of Computer Science, Central China Normal University, Wuhan, China, in 2006. She is currently pursuing the Ph.D. degree with Fujian Normal University, Fuzhou, China. She is also a Lecturer with the College of Computer and Cyber Security, Fujian Normal University. Her research interests include complex networks, social networks, graph theory and application, network analysis, and fault diagnosis.

WEI LIN received the M.S. degree in mathematics from the South China University of Technology, in 2014. She is currently a Lecturer with Fujian Normal University. Her research interests include community detection, fault-tolerant computing, and social networks.

QIANRU ZHOU received the B.S. degree from the School of Mathematics and Information, Fujian Normal University, Fuzhou, China. She is currently pursuing the M.S. degree with the School of Mathematics and Statistics, Fujian Normal University. Her research interests include connectivity, Hamiltonian laceability, fault diagnosis, graph theory and application, and social networks.